Popel, Johnson (eds.), Microvascular Networks: Experimental and Theoretical Studies. Symp., Tucson, Ariz., 1985, pp. 197–209 (Karger, Basel 1986)

# Hemodynamic Significance of Microvascular Arteriolar Anastamosing

*Harvey N. Mayrovitz*

Research Division, Miami Heart Institute, Miami Beach, Fla., USA

Descriptions of arteriolar-arteriolar connections (A-A) within the microvasculature are numerous. According to Krogh [8], 'Branches of supplying arteries anastomose forming a primary network. Into these meshes small arteries are given off at regular intervals, and these again anastomose freely. Arterioles then branch off at regular intervals and finally split into a large number of capillaries....' Similar observations have been made by others. Zweifach [20] noted that '...a striking feature of skeletal muscle, intestinal wall and skin is the presence of extensive cross-connections between small arteries and arterioles which form a series of arcades'. Baez [1], in describing the cremaster microvasculature, observed that '...arterial side branches run radially from the parent vessel and after giving off numerous arterioles anastomose with similar vessels... an extensive anastamotic network is found to the fourth or fifth order of branches from the main vessel..'

In spite of the ubiquitous presence of A-A, their function is speculative and little quantitative work has been done to estimate their hemodynamic significance. Based on observations in the bat wing, Nicoll and Webb [16] stated that: 'Arterioles form concentric arcuate patterns that by their structure and functional adaptation insure nearly equal and adequate pressure and volume conditions at the heads of terminal arterioles.' A similar view was put forward by Zweifach [20]: 'The interarcading patterns is believed to represent a means of equalizing pressure relationships and the distribution of blood within the tissue.'

Intuitively, the functional attributes assigned to A-A by these workers seem to be close to the mark. But, clarification of fundamental issues remain undone. What is the source and extent of hemodynamic nonuniformity that A-A are speculated to ameliorate? What are the microvascular

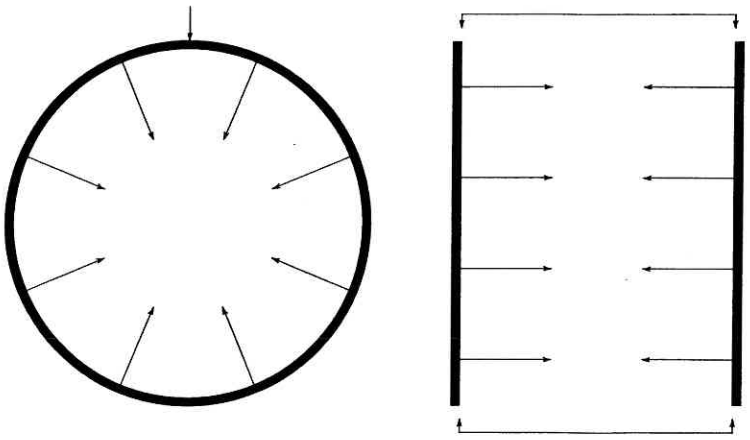

*Fig. 1.* Alternate representations of an arteriolar distribution to a tissue region. The arcuate pattern on the right may be viewed as the ladder-like pathways on the left with inlet and outlet ports joined.

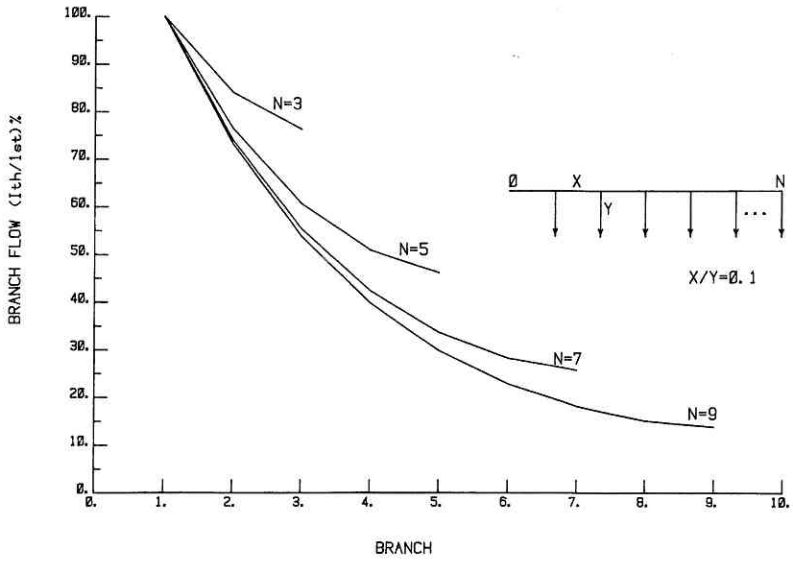


*Fig. 2.* Branch flow nonuniformity in a uniform resistance ladder pathway. Interbranch resistances (X) and branch input resistances (Y) are uniform. Data are for X/Y=0.1.

parameters that effect the amount of nonuniformity and to what extent do A-A in fact alter these? In what follows an attempt will be made to characterize some of the features of the microvascular network which bear importantly on these questions.

*Sources of Hemodynamic Nonuniformity*

Physiological control mechanisms are powerful sources for producing temporal and spatial hemodynamic changes within the microvasculature. This control is exercised within the confines of a microvascular network of a given topography principally via adjustment of vessel diameter. The effect of these mechanisms on pressure and flow distribution have been dealt with previously [10, 13]. In the present report physiological control as it relates to either increasing or decreasing hemodynamic nonuniformity is not dealt with. Rather, the structure of the network itself and its relationship to pressure and flow distribution is the primary concern.

Two network 'forms' for supplying the needs of a given tissue region are illustrated schematically in figure 1. The circular blood distribution network with uniform spoke-like branches supplying the tissue conforms to Nicoll and Webb's description, and appears ideal in the sense it appears to provide equal pressure at the heads of the arterioles. But, as drawn in the other half of the figure, the same network is seen to consist of uniform pathways joined at the proximal and distal ends. When drawn in this fashion, the 'ladder-like' structure of the arteriolar network is more clearly revealed, and the dependence of pressure and flow distribution on the parameters of the parent vessel and its branches becomes more apparent.

Consider, for example, the uniform ladder network in figure 2. Uniform here means that each interbranch resistance, X, and each branch input resistance, Y, is equal. A comparison of the flow in each of the branches relative to the flow in the first branch reveals a dramatic and progressive flow decrement. The flow and pressure attenuation depends on X/Y and the number of branches, as listed in table I. Each entry is the pressure or flow at each branch expressed as a percentage of its corresponding value at the first branch. At each node, the corresponding pressures and branch flows normalized in this fashion are equal for this model. From the calculated results of table I, one may conclude that depending on the in vivo values of X/Y, the uniform ladder structure may give rise to significantly nonuniform pressure and flow distributions.

*Table I.* Pressure and flow distribution along ladder-like pathways

| X/Y | n | Branch | | | | | | | | |
|---|---|---|---|---|---|---|---|---|---|---|
| | | No. 2 | No. 3 | No. 4 | No. 5 | No. 6 | No. 7 | No. 8 | No. 9 | No. 10 |
| 0.01 | 4 | 97 | 95 | 94 | | | | | | |
| | 6 | 95 | 92 | 89 | 88 | 87 | | | | |
| | 8 | 94 | 89 | 85 | 82 | 80 | 78 | 77 | | |
| | 10 | 93 | 87 | 82 | 78 | 74 | 71 | 69 | 68 | 67 |
| 0.02 | 4 | 95 | 91 | 89 | | | | | | |
| | 6 | 92 | 83 | 81 | 78 | 76 | | | | |
| | 8 | 90 | 81 | 75 | 70 | 66 | 63 | 62 | | |
| | 10 | 89 | 79 | 71 | 64 | 59 | 55 | 52 | 50 | 49 |
| 0.04 | 4 | 90 | 83 | 80 | | | | | | |
| | 6 | 86 | 75 | 68 | 63 | 60 | | | | |
| | 8 | 84 | 71 | 61 | 53 | 48 | 45 | 43 | | |
| | 10 | 83 | 69 | 58 | 49 | 42 | 37 | 33 | 31 | 29 |
| 0.08 | 4 | 82 | 71 | 66 | | | | | | |
| | 6 | 78 | 62 | 51 | 44 | 41 | | | | |
| | 8 | 77 | 59 | 46 | 36 | 30 | 26 | 24 | | |
| | 10 | 76 | 57 | 44 | 34 | 26 | 21 | 17 | 15 | 14 |

Entries are pressure and flows as a percent of values in branch No. 1.
X is parent vessel interbranch resistance and Y is the input resistance of each of the n branches.

The nonuniformity is amplified when multiple ladder-like pathways are coupled into a network. The genesis of this amplification is illustrated in figure 3. A single arteriolar vessel is shown giving rise to five branches, each of which in turn give rise to seven branches. The pressure P5, which serves as the input to the fifth branch, is reduced to 46% of the entrance pressure P1. The distribution of P5 to its dependent branches is subsequently further attenuated by an amount determined by the number of branches and the parameters of the ladder pathway. Until now these parameters have been assigned on the basis of uniform segmental and branch resistances appropriate for a given branching order. It should be clear that no in vivo network meets these criteria but the extent of departure has never been quantified. Nonetheless, the 'uniform resistance' model has so far served us well in sorting out the general network features.

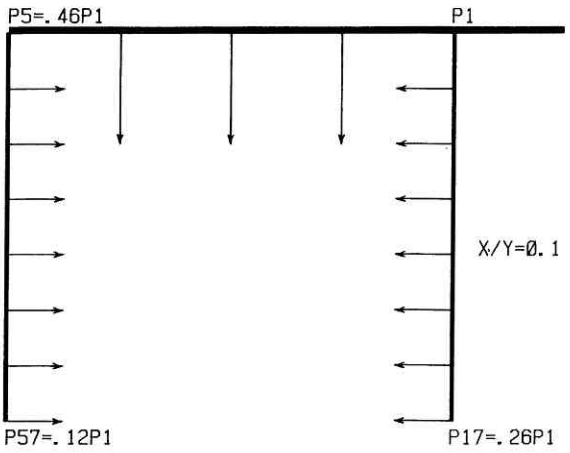


*Fig. 3.* Nonuniformity amplification due to coupling of ladder pathways. The parent vessel input pressure P1 is progressively attenuated resulting in decreased input pressure to the branches. The attenuation is amplified through the branch pathways.

An additional possibility to consider is that at some levels (terminal arteriole-capillary) the ladder pathways may be more likely to produce uniform flow to the branches. The parameters of such a network (uniform 'Q') are compared with those of a uniform 'R' in figure 4. Note that in this figure J=1 corresponds to the most distal branch. If as a boundary condition the flows in the most distal branches (J=1) are assumed equal, then it can be shown that each branch of the uniform 'Q' network will have this flow if the branch resistances increase in accordance with the relationship $(R(J)=Y[1+J(J-1)(X/2Y)]$, J = 1 to N. For the seven branch network illustrated in the figure the uniform 'R' model requires significantly more total flow to realize the same end flow requirement. These results show that ladder-like structures need not give rise to flow nonuniformity. The type of flow distribution they produce is strictly a function of the parameter values .

*Extension to Full Network Model*

As noted, the parameters of the composite set of pathways comprising a given microvascular network determine the A-A hemodynamic significance. Thus, for further insight regarding A-A effects we now focus on a specific network model.

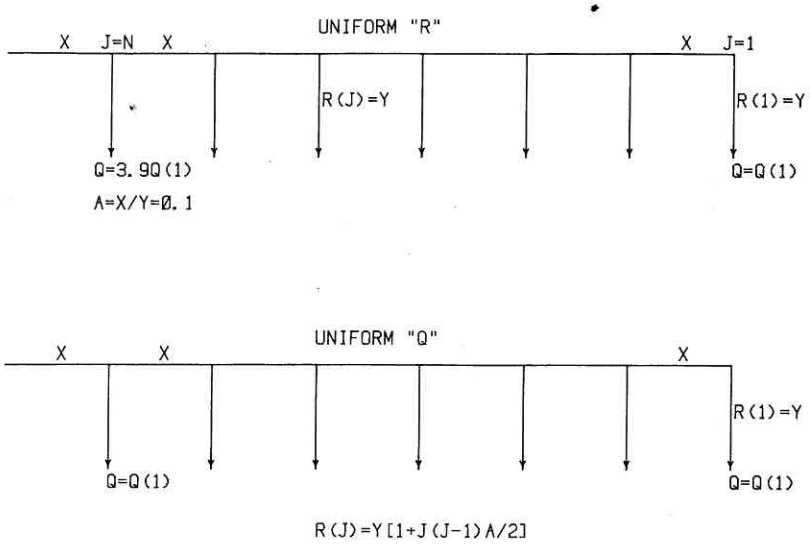


*Fig. 4.* Uniform branch flow achieved via non-uniform branch resistances. In the uniform 'R' model all branches have equal resistance but flow is nonuniform. In the uniform 'Q' model branch resistances increase from the distal end such that all flows are equal. R(J) denotes the input resistance of the Jth branch measured from the downstream end.

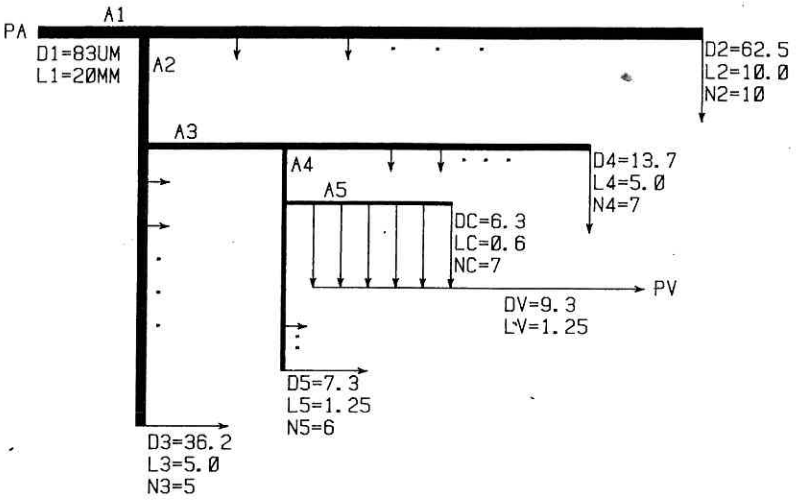


*Fig. 5.* Network model of the rat cremaster microvasculature used as basis for evaluating effects of A-A. Numerical data for vessel diameters (D), lengths (L) and number of branches (N) from several authors, as described in the text.

Figure 5 is a schematic representation of the rat cremaster muscle microvasculature. This model is not intended to reproduce all of the complex topographical detail associated with the real microvasculature. It includes a level of detail judged to be adequate to estimate A-A effects under conditions resembling the multiple in vivo pathways. Numerical data for vessel diameters (D), lengths (L) and number of branches (n) have been compiled from the works of the several authors. Arteriolar diameters are based on the data from Roy and Mayrovitz [17]. Capillary diameter is based on the data from Chen and Prewitt [4]. Venule diameter is based on the data of Bohlen et al. [2]. Capillary length is based on the data of Smaje et al. [19]. Arteriolar lengths are based on the data of Hutchins and Darnell [6], Dusseau and Hutchins [5], and Roy and Mayrovitz [18]: Number of branches at the various levels is based on the data of Hutchins and Darnell [6], Chen et al. [3], and data from the author's laboratory.

The cremaster is modeled to have five arteriolar branching orders (A1–A5) with the A5 level directly feeding the capillaries. Each capillary arising from the same A5 is modeled to drain into the same venule. Each vessel and its $N_i$ branches are modeled as ladder pathways. The interbranch resistances ($X_j$) are calculated on the basis of Poiseuille's equation and the shunt pathway resistance ($Y_j$) is the input resistance of the next branching order [11].

Branching order dependent hematocrit differences [7, 9] are included in the present model by first estimating local hematocrit relative to systemic hematocrit by the linear regression equation $H_r = 0.00966D + 0.140$ with D in μm [15]. Since systemic hematocrit for the rat averages about 40% [14], the local microvessel fractional red blood cell concentration was estimated based on the equation $H_\mu = 0.0039D + 0.056$ with D in μm. From the values of $H_\mu$ calculated from this equation, the local microvessel blood viscosity, $V_\mu$, was then estimated from the equation [12]:

$$V_\mu = V_p \{1 + 2.5 [H_\mu/(1 - H_\mu)]\} \qquad (1 - H_\mu)$$

in which $V_p$ is the plasma viscosity taken here as 1.28 cP.

The model is first used to estimate the effect of arteriolar-arteriolar anastomoses between A2 vessels (A2-A2) on the input resistance of the entire microvascular network. For convenience of representing these results, it is useful to view the entire network in a reduced form as shown in figure 6 in which flow enters the network from the right at the site labeled GIN. This site corresponds to the site labeled PA in figure 5. The N = 10 branch path-

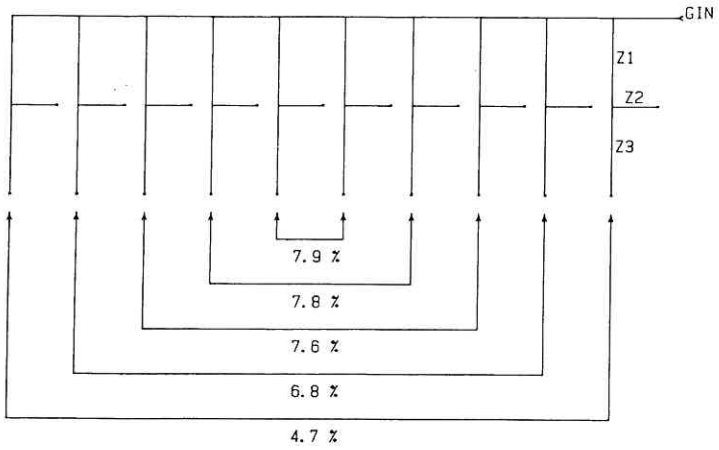


*Fig. 6.* Reduced model of cremaster microvasculature. Ten branch pathways originating from the main A1 are each characterized as equivalent 'T'. The lines with arrows represent interconnecting loops (A-A) placed progressively and cumulatively between the first and last remaining unlooped branches. Numbers are the percentage increase in vascular bed input conductance (GIN) as compared with no A-A present.

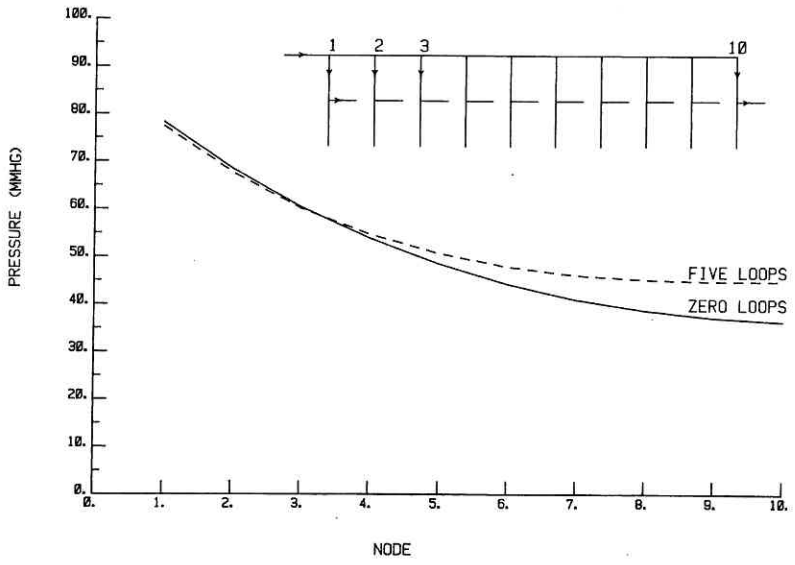


*Fig. 7.* Pressure distribution along an A1 vessel. The presence of all five loops is shown to slightly decrease the progressive pressure attenuation.

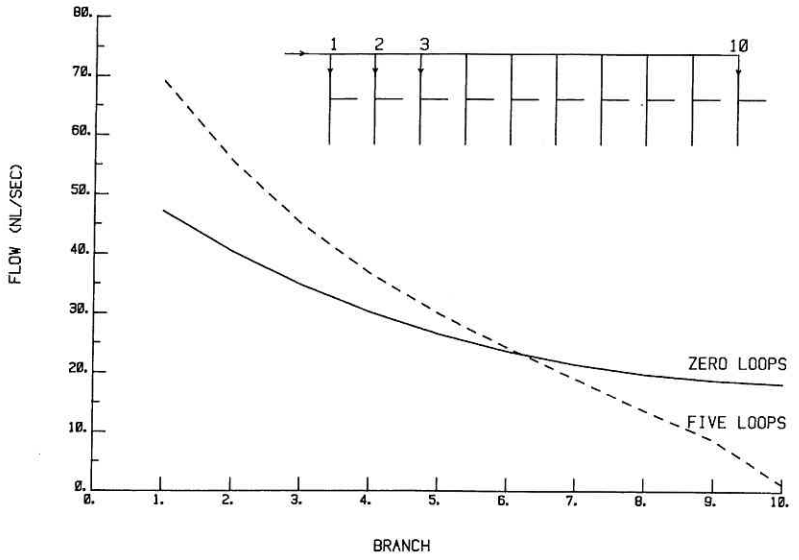


*Fig. 8.* Flow distribution from an A1 vessel. Branch flows entering from the parent A1 vessel are seen to become more nonuniform with A2-A2 presence. Upstream flows are greater and downstream flows are less than with no A2-A2 present.

ways originating from the A1 vessel of figure 5 are represented as 'T' sections of classic circuit analysis theory. Each section characterizes the vascular network distal to the junction with the A1. The parameters Z1, Z2 and Z3 are determined by analyzing the full network embodied in figure 5 and are equal to 3.09, 11.4 and 2.03 $\times$ $10^5$ mmHg/ml/s, respectively. The A1 interbranch resistance is 0.42 $\times$ $10^5$ mmHg/ml/s. Values are based on local calculated viscosities of 3.24, 2.65, 2.07, 1.67, 1.58, 1.56 and 1.61 cP for A1 vessel through venule, respectively.

To determine the effect of A2-A2, the input conductance (GIN) was determined without, and then with, the presence of A-A. This input conductance without A-A that which would be calculated from the model shown in figure 5 as the total flow entering A1, divided by PA-PV. This would also be the value of GIN in figure 6 with no A-A in place. The value of GIN with A-A present would similarly be calculated from the model of figure 5 but under conditions in which the distal end of a specified A2 vessel in connected to the distal end of a different A2 vessel. The placement sites of A2-A2 and the effect of the A-A on GIN is shown in figure 6. In this figure, the percentage increase in GIN due to a single A2-A2 between the first and tenth (last)

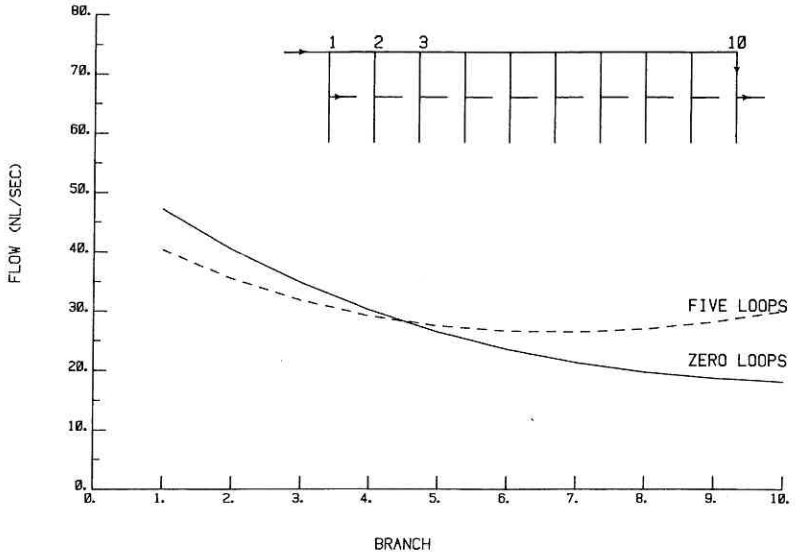


*Fig. 9.* Flow distribution to the distal microvasculature. The presence of A2-A2 tends to even out the flow perfusing the distal microvasculature (shown as horizontal arrows in 'T' sections).

branch is shown as 4.7%. This was the largest change attributale to a single A2-A2. This A2-A2 was left in place and other A2-A2 were progressively added (and left in place) to determine the summated effect of multiple A2-A2. With all five A-A in place the input conductance was determined to be 7.9% greater than if no A-A were present.

Figure 7 shows the pressures that would be measured at different sites along the A1. The pressure along the A1 in the absence of A2-A2 (zero loops) decreases from an input pressure of 90 mm Hg to 36 mm Hg at the most distal site. Presence of five A2-A2 (five loops) buffer this fall in pressure slightly but a significant gradient of pressure along A1 remains.

Figure 8 shows the flow that would be measured entering consecutive branch pathways arising from A1. Branch flows progressively decrease along the A1. With no A2-A2 present the first branch flow of 47 nl/s is decreased to 19 nl/s at the tenth branch pathway. The presence of the five A2-A2 increases this flow nonuniformity and results in a greater flow entering the proximal branches but a lesser flow entering the more distant branches. However, as shown in figure 9, the actual flow to the dependent distal microvasculature (shown as the horizontal arrows in the center sections of the 'T') is in fact

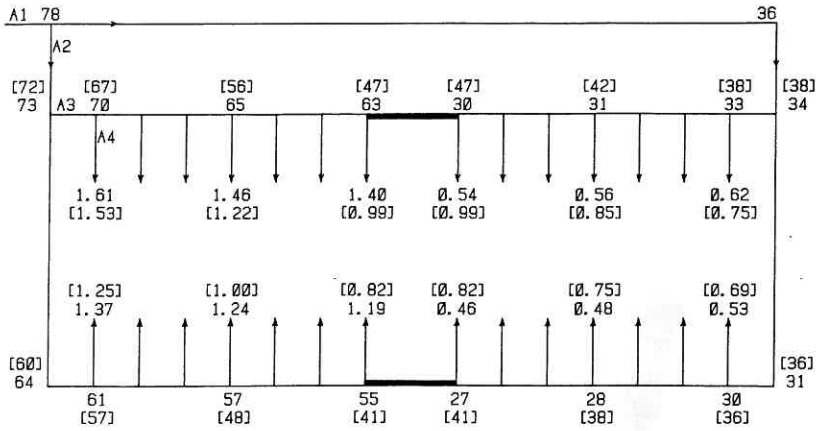


*Fig. 10.* Pressure and flow distributions as influenced by branch origin site and A3-A3 presence. Numbers in brackets apply when the A-A (thick solid lines) are in place. The two digit numbers are pressures (mm Hg), and all other numbers are flows (nl/s).

made more uniform as a consequence of the A2-A2 presence. This occurs because the distal flow is the sum of the flows that enter a branch directly from the A1 parent and the flow that enters the branch via the A-A. In the more proximal branches (1–4) the prevailing pressure gradients provide flow directly only from the A1 vessel. In the branches further downstream, the distal vasculature receives flow via the A-A as well.

The composite results illustrated in figures 6–9 show that as a consequence of multiple A-A between higher order arteriolar vessels there results: (1) a slight reduction in input resistance; (2) a slight buffering of the normal pressure fall-off along the main arteriolar vessels; (3) a considerable increase in the nonuniformity of flow entering A2 pathways, and (4) a moderate increase in the uniformity of the flow perfusing the distal vasculature (A3 and beyond).

As a final point, it is instructive to examine in greater detail the effects of A-A which occur at more distal sites. For this purpose A-A between A3 vessels are considered, as illustrated in figure 10. For simplicity this figure shows in detail only four A3 pathways with corresponding A4 branches. These A3 pathways are the first and fifth (last) branches originating from the first and

tenth (last) A2 branches of figure 5. The two thick solid lines linking the terminal nodes of each A3 vessel in figure 10 represent A3-A3 anastomoses. Numbers without brackets are the network pressures (at nodes) in mm Hg and flows (at arrows) in nl/s calculated without A3-A3. Corresponding pressures and flows with the A3-A3 in place are shown within the brackets. The following general features are illustrated by the data obtained from this network model.

*Without A-A*

Pressures and corresponding flows into A4 branches that originate from the same A3 vessel differ by at most 13%. But, the pressures and flows along those A3 vessels which originate from the distal A2 branch are at most one-half that measured in corresponding branches of the proximal A2 vessel. Thus, when the pathway parameters are fixed, the major source of pressure and flow nonuniformity is related to the location of the branch pathway origin.

*With A-A*

The presence of A-A force pressure equivalance between the terminal nodes of the linked A3 vessels. In general, the common pressure at this union is approximately the mean of the pressures that would be present without A-A. Thus, due to A3-A3 presence, pressures in the A3 vessels originating from the upstream A2 vessel decrease while pressures in the A3 vessels originating from the downstream A2 vessel increase. As a consequence a more uniform pressure distribution along the now linked A3-A3 vessel is achieved and there results a more uniform perfusion of the corresponding A4 branch pathways.

## *References*

1 Baez, S.: Skeletal muscle and gastrointestinal microvascular morphology; in Kaley, Altura, Microcirculation, vol. 1, pp. 69–74 (University Park Press, Baltimore 1977).
2 Bohlen, H.G.; Gore, R.W.; Hutchins, P.M.: Comparison of microvascular pressures in normal and spontaneously hypertensive rats. Microvasc. Res. *13:* 125–130 (1977).
3 Chen, I.I.H.; Prewitt, R.L.; Dowell,. R.F.: Microvascular rarefaction in spontaneously hypertensive rat cremaster muscle. Am. J. Physiol. *241:* H306–H310 (1981).
4 Chen, I.I.H.; Prewitt, R.L.: Capillary pressure gradients in cremaster muscle of normotensive and spontaneously hypertensive rats. Microvasc. Res. *25:* 145–155 (1983).

5 Dusseau, J.W.; Hutchins, P.M.: Stimulation of arteriolar number by salbutamol in spontaneously hypertensive rats. Am. J. Physiol. *236:* H134-H140 (1979).
6 Hutchins, P.M.; Darnell, A.E.: Observation of a decreased number of small arterioles in spontaneously hypertensive rats. Circulation Res. *34:* I-161–I-165 (1974).
7 Klitzman, B.; Duling, B.R.: Microvascular hematocrit and red cell flow in resting and contracting striated muscle. Am. J. Physiol. *237:* H481–H490 (1979).
8 Krogh, A.: The anatomy and physiology of capillaries (Yale University Press, New Haven 1922).
9 Lipowsky, H.H.; Usami, S.; Chien, S.: In vivo measurements of apparent viscosity and microvessel hematocrit in the mesentery of the cat. Microvasc. Res. *19:* 297–319 (1980).
10 Mayrovitz, H.N.; Wiedeman, M.P.; Noordergraaf, A.: Microvascular hemodynamic variations accompanying microvessel dimensional changes. Microvasc. Res. *10:* 322–339 (1975).
11 Mayrovitz, H.N.; Wiedeman, M.P.; Noordergraaf, A.: Analytical characterization of microvascular resistance distribution. Bull. Math. Biol. *38:* 71–82 (1976).
12 Mayrovitz, H.N.; Tuma, R.F.; Wiedeman, M.P.: Relationship between microvascular blood velocity and pressure distribution. Am. J. Physiol. *232:* H400–H405 (1977).
13 Mayrovitz, H.N.; Wiedeman, M.P.; Noordergraaf, A.: Interaction in the microcirculation, in Baan, Noordergraaf, Raines, Cardiovascular system dynamics, pp. 194–204 (MIT Press, Cambridge 1978).
14 Mayrovitz, H.N.; Polani, A.; Tatarsky, S.; Roy, J.: Blood viscosity: a non-factor in spontaneous hypertension. Proc. Annu. Conf. Eng. med. Biol. *24:* 169 (1982).
15 Mayrovitz, H.N.; Roy, J.: Microvascular blood flow. Evidence indicating a cubic dependence on arteriolar diameter. Am. J. Physiol. *245:* H1031–H1038 (1983).
16 Nicoll, P.A.; Webb, R.: Vascular patterns and active vasomotion as determiners of flow through minute vessels. Angiology *6:* 291–308 (1955).
17 Roy, J.; Mayrovitz, H.N.: Microvascular blood flow in the normotensive and spontaneously hypertensive rat. Hypertension *4:* 264–271 (1982).
18 Roy, J.; Mayrovitz, H.N.: Microvascular pressure, flow and resistance in spontaneously hypertensive rats. Hypertension *6:* 877–886 (1984).
19 Smaje, L.; Zweifach, B.W.; Intaglietta, M.: Micropressures and capillary filtration coefficients in single vessels of the cremaster muscle of the rat. Microvasc. Res. *2:* 96–110 (1970).
20 Zweifach, B.W.: Functional behavior of the microcirculation (Thomas, Springfield 1961).

Dr. Harvey N. Mayrovitz, Miami Heart Institute, 4701 N. Meridian Avenue,
Miami Beach, FL 33140 (USA)